Photoacoustics 25 (2022) 100335

Contents lists available at ScienceDirect

Photoacoustics

journal homepage: www.elsevier.com/locate/pacs

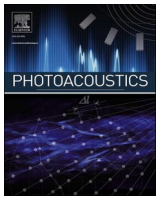

# Detection of weak optical absorption by optical-resolution photoacoustic microscopy

Tingyang Duan [a,b,c,1], Xiaorui Peng [a,c,1], Maomao Chen [a,1], Dong Zhang [a,c,1], Fei Gao [b,*,1], Junjie Yao [a,*,1]

[a] Department of Biomedical Engineering, Duke University, Durham, NC 27708, USA
[b] Hybrid Imaging System Laboratory, Shanghai Engineering Research Center of Intelligent Vision and Imaging, School of Information Science and Technology, ShanghaiTech University, Shanghai, China
[c] Departmentof Biomedical Engineering, Tsinghua University, Beijing 100084, China

ARTICLE INFO

*Keywords:*
Optical-resolution photoacoustic microscopy
Detection sensitivity
Limited detection view
Limited detection bandwidth
Nonlinear effect
Molecular imaging

ABSTRACT

Optical-resolution photoacoustic microscopy (OR-PAM) is one of the major implementations of photoacoustic (PA) imaging. With tightly focused optical illumination and high-frequency ultrasound detection, OR-PAM provides micrometer-level resolutions as well as high sensitivity to optical absorption contrast. Traditionally, it is assumed that the detected PA signal in OR-PAM has a linear dependence on the target's optical absorption coefficient, which is the basis for quantitative functional and molecular PA imaging. In this paper, we demonstrate that, due to the limited detection bandwidth and detection view, OR-PAM can have a strong nonlinear dependence on the optical absorption, especially for weak optical absorption ($<10$ cm$^{-1}$). We have investigated the nonlinear dependence in OR-PAM using numerical simulations, analyzed the underlining mechanisms, proposed potential solutions, and experimentally confirmed the results on phantoms. This work may correct a traditional misunderstanding of the OR-PAM signals and improve quantitative accuracy for functional and molecular applications.

## 1. Introduction

Photoacoustic imaging (PAI) is a non-invasive biomedical imaging technique that combines the merits of rich optical absorption contrast and deep ultrasound detection [1–6]. In PAI, acoustic waves are generated by transient light absorption and thermoelastic expansion [7,8]. An ultrasonic transducer or transducer array detects the acoustic waves, and forms an image that maps the original optical energy deposition. As an optical imaging modality, PAI is sensitive to the optical absorption contrast. It is traditionally accepted that a small percentage change in the optical absorption coefficient leads to the same percentage change in the detected PA signal amplitude [6], which provides the foundations for functional and molecular sensitivity, such as quantifying oxygen saturation of hemoglobin ($sO_2$) [9–11]. Depending on the image formation methods, PAI has two major implementations: photoacoustic microscopy (PAM) [12] and photoacoustic computed tomography (PACT) [4,13]. Optical-resolution PAM (OR-PAM) is a major PAM implementation, which provides high spatial resolution by using tightly focused optical excitation and high-frequency acoustic detection. OR-PAM is most often implemented in the reflection mode, using an optical-acoustic beam combiner to achieve confocal and co-axial alignment of the optical excitation and acoustic detection [6,12,14]. The optical-acoustic beam combiner usually limits the numerical aperture of the optical focusing lens to be ~0.1 [15–17]. OR-PAM with a higher numerical aperture needs to be configured in the transmission mode [16,18] or off-axis mode [19], which, however, has difficult to image bulky tissues or thick samples.

In OR-PAM, it is similarly assumed that the detected PA signal's amplitude is proportional to the optical absorption coefficient of the target ($\mu_a$). However, this simple assumption may not be true in some special conditions. Danielli et al. have shown that there exists optical absorption saturation effect in OR-PAM with strong optical fluence, due to the depletion of the ground state electrons [20–22]. Wang et al. have demonstrated that the detected PA signal saturates with large $\mu_a$, due to the reduced penetration depth of photons [23]. In this work, we report another nonlinear effect in OR-PAM when detecting small $\mu_a$ or weak

* Corresponding authors.
*E-mail addresses:* gaofei@shanghaitech.edu.cn (F. Gao), junjie.yao@duke.edu (J. Yao).
[1] These authors contributed equally to this work.

https://doi.org/10.1016/j.pacs.2022.100335
Received 30 August 2021; Received in revised form 4 February 2022; Accepted 4 February 2022
Available online 7 February 2022

optical absorption, mainly due to the ultrasonic transducer's limited detection bandwidth and limited view angle. This effect may result in missing structures in OR-PAM images and inaccurate quantification of functional parameters or molecular probes. To investigate the nonlinear dependence on optical absorption in OR-PAM, we first simulated the PA signals with various optical absorption coefficients and different detection orientations. The numerical results have clearly demonstrated the nonlinear signal dependence when the numerical aperture of the optical focusing is small and the optical absorption of the target is weak. We also performed phantom experiments with different detection schemes, and the experimental results agreed well with the simulation results. We expect that this study may provide useful information for improving the detection sensitivity and quantification accuracy of OR-PAM in functional and molecular imaging.

## 2. Theories and simulations

We have recently demonstrated that OR-PAM, despite its tight optical focusing, can have the limited-view issue, similar to PACT [15,24]. Due to the coherent photoacoustic signal generation within the excited target volume [25,26], the focused ultrasound transducer in OR-PAM cannot receive the PA signals generated by the structures aligned with the transducer's acoustic axis, i.e., vertical structures. In other words, with the focused optical illumination and acoustic detection that are coaxially aligned, OR-PAM is not able to detect acoustic waves propagating parallel to the optical beam axis. One consequence of the limited-view issue is the missing vertical structures in OR-PAM, such as the diving vessels in the mouse brain, as reported previously [25,26]. Another consequence of the limited-view issue is the nonlinear signal dependence on the weak optical absorption of the target. In reflection-mode OR-PAM systems with a small numerical aperture (e.g., 0.1), the focused excitation beam has an elongated Gaussian shape, with the depth of focus (e.g., 65 μm) much longer than the beam width (*e.g.*, 4 μm). Within the focused excitation volume, the optical attenuation can be described by the Beer-Lambert law. The optical absorption coefficient of the target determines the penetration depth of light and thus the effective excitation volume or shape. Strong optical absorption leads to a low penetration depth and thus a small target size along the beam axis, which results in isotropically-propagating spherical waves, as shown in Fig. 1a. By contrast, weak optical absorption leads to a relatively large penetration depth and thus a long target size along the beam axis, which results in side-propagating cylindrical ultrasound waves (Fig. 1a). In other words, a target with weak optical absorption is more like a vertical structure for the ultrasound transducer placed on top of the target, and thus is less likely to be detected. The limited view issue in OR-PAM results in the nonlinear dependence of the detected PA signals on the weak optical absorption.

With pulsed laser excitation that satisfy the thermal and stress confinement [27], the acoustic frequency spectrum of the generated PA signals depends on the target size [26,28–30]. Approximately, a larger target size leads to PA signals with lower frequency components, and vice versa. Again, in OR-PAM, the weak optical absorption of the target results in a longer penetration depth of the light, and thus a larger target size along the beam axis Therefore, the acoustic waves generated by weakly absorbing targets (and thus larger target size) have stronger low-frequency components, and vice versa. However, the ultrasonic transducer often has a limited detection bandwidth (typically less than 100% of the central frequency), and thus cannot always match the signal frequency spectra from targets with different sizes. As we will show below, when the optical absorption is low ($<10$ cm$^{-1}$), the generated PA signal frequencies along the optical beam axis concentrate around 10–15 MHz, which is typically outside the detection bandwidth of the ultrasound transducer in OR-PAM. The mismatched detection bandwidth becomes the second contributor to the nonlinear effect.

In order to investigate the nonlinear effect induced by the limited-view and limited-bandwidth in OR-PAM, we performed numerical simulations using the *K-wave* toolbox in Matlab [31,32]. All the simulation parameters were based on a typical reflection-mode OR-PAM system. The simulation setup is shown in Fig. 1b, in which a 300-μm-diameter tube was filled with absorbing medium as the PA target. A focused Gaussian laser beam (NA: 0.1) was the excitation light source. The focus of the Gaussian beam was placed 80 μm below the tube top surface, and the optical attenuation inside the tube was computed based on the Beer's law. A spherically focused ultrasonic transducer (central frequency, 30 MHz; −6 dB bandwidth, 100%; NA, 0.5) was placed on top of the laser beam to simulate the reflection-model OR-PAM. As the control study, we also simulated an identical transducer placed on the side of the laser beam. Both transducers were confocally aligned with the focused light beam, with an acoustic focal length of 6 mm. For the comparison purpose, we recorded PA signals both with and without applying the transducer's detection bandwidth.

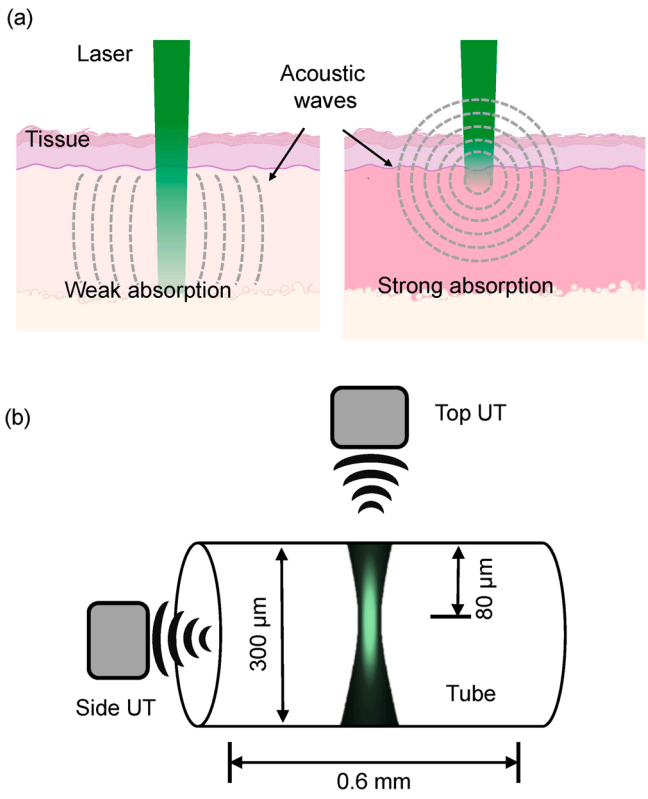


**Fig. 1.** Principle of the nonlinear dependence of OR-PAM on weak optical absorption. (a) Schematics of OR-PAM signal generation and propagation with weak and strong optical absorption. (b) Schematics of the k-wave simulation. The laser beam is focused 80 μm into a 300-μm-diameter tube filled with absorbing medium. The resultant PA waves are detected both on the top and on the side of the laser beam. UT, ultrasound transducer.

Firstly, we demonstrated the drastically different photoacoustic wave propagation in OR-PAM with strong and weak optical absorption. As shown in Fig. 2a, when the target had weak optical absorption ($\mu_a = 0.1$ cm$^{-1}$), the generated PA waves were behaving like cylindrical waves, with most of the energy travelling sideways. The PA wave pressure arriving at the top transducer was ~4 times weaker than that at the side transducer. This is a classic limited-view example in reflection-mode OR-PAM, leading to the low visibility of the weakly-absorbing targets. As a comparison, when the target had strong optical absorption (200 cm$^{-1}$), the generated PA waves were behaving like spherical waves, with the energy distributed more uniformly along all directions (Fig. 2b). The PA wave pressure at the top and side transducer has only ~5% difference. Therefore, the weak optical absorption can induce more severe limited-view issue in OR-PAM, while the strong optical absorption can help mitigate this problem.

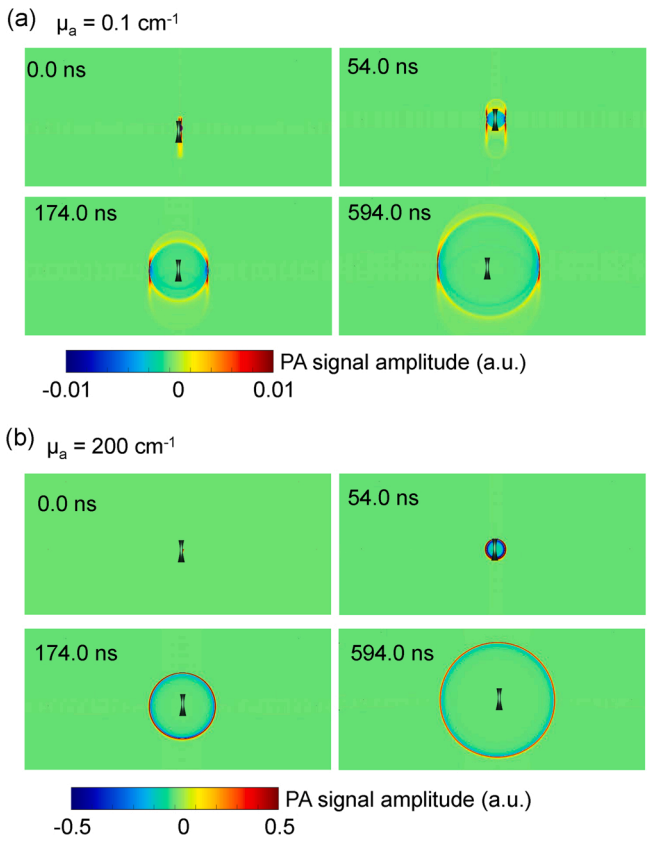


**Fig. 2.** Simulated PA wave propagation with weak and strong optical absorption. (a) Snapshots of the wave propagation with $\mu_a = 0.1$ cm$^{-1}$, showing the side-travelling cylindrical waves. (b) Snapshots of the wave propagation with $\mu_a = 200$ cm$^{-1}$, showing the isotropically-travelling spherical waves.

We simulated a wide range of optical absorption coefficients from 0.01 to 300 cm$^{-1}$ and compared the detected PA signal amplitudes by the top and side transducers, as shown in Fig. 3a. The first important observation is that the PA signal amplitudes detected by the top transducer have a clear nonlinear dependence on the absorption coefficient. The detected PA signals saturate as the absorption becomes stronger, which is consistent with the previously reported results on acoustic-resolution PAM [23]. Even when the optical absorption is weak (<10 cm$^{-1}$), the saturation effect is still present, as shown in Fig. 3a. Such a saturation effect is mainly resultant from the limited detection bandwidth of the ultrasound transducer. To confirm the origin of the signal saturation, we analyzed the frequency spectrum of the PA signals arriving at the transducer. As the optical absorption increases, the frequency spectrum of the generated PA signal shifts to higher frequencies, leading to reduced detection sensitivity by the band-limited transducers. For example, with weak optical absorption of 0.1 cm$^{-1}$, the central frequency of the PA signal at the top transducer is ~19 MHz, which is within the detection bandwidth of the transducer. However, with strong optical absorption of 200 cm$^{-1}$, the central frequency of the PA signal is shifted to 48 MHz, which is beyond the detection bandwidth of the transducer.

The second observation is that the PA signal amplitude detected by the top transducer is much lower than the side transducer when the optical absorption is weak (≤10 cm$^{-1}$) (Fig. 3a). For example, at 10 cm$^{-1}$, the side transducer signal is 5 times of the top transducer signal (Fig. 3a). This is mainly because of the limited-view issue as discussed above, in which the top transducer cannot detect the side-travelling cylindrical waves when the optical absorption is weak. Meanwhile, Fig. 3b shows the difference in the central frequency of the PA signals from the weakly absorbing targets, detected by the top and side

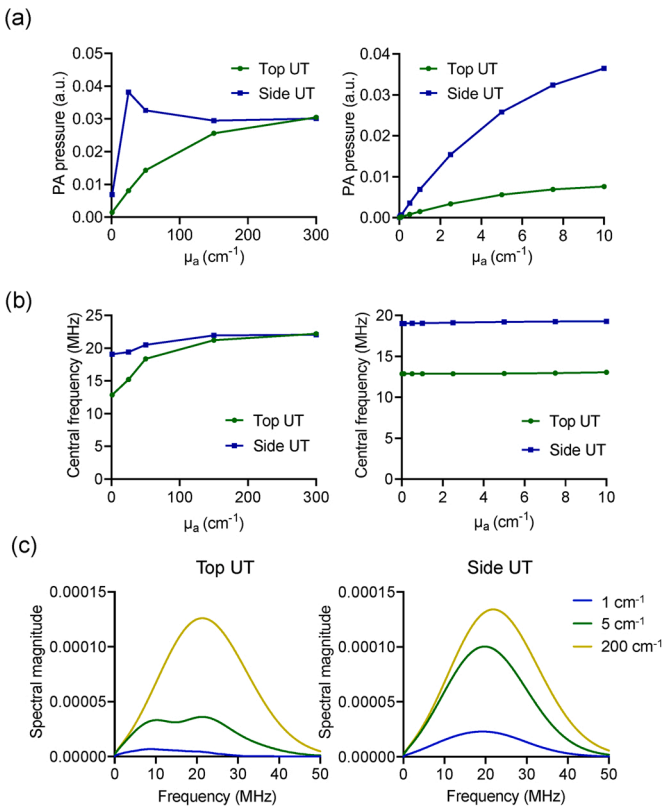


**Fig. 3.** Simulated PA signals detected by top and side transducers. (a) Left, the PA signal amplitudes detected by the top and side transducers as the optical absorption coefficient varies from 0.05 cm$^{-1}$ to 300 cm$^{-1}$. Right, a close-up plot of the signal amplitudes with weak optical absorptions of ≤ 10 cm$^{-1}$. (b) Left, the central frequency of the detected PA signals as the optical absorption varies from 0.05 cm$^{-1}$ to 300 cm$^{-1}$. Right, a close-up plot of the signal central frequency with weak optical absorptions of ≤ 10 cm$^{-1}$. (c) Frequency spectra the detected PA signals by the top and side transducers, with optical absorptions of 1 cm$^{-1}$, 5 cm$^{-1}$ and 200 cm$^{-1}$.

transducers. Fig. 3c shows the representative frequency spectra with different optical absorption. The top transducer receives lower frequencies than the side transducers because of the cylindrical shape of the excited volume. This result also indicates that, with the same detection bandwidth centered around 30 MHz, the side transducer is more efficient than the top transducer in detecting the signals from weakly absorbing targets. When the optical absorption is strong (≥200 cm$^{-1}$), there is virtually no difference between the top and side transducers, because the generated PA signals travel as spherical waves. It is interesting to observe that the side transducer signal amplitude decreases when the optical absorption increases from 10 cm$^{-1}$ to 300 cm$^{-1}$. This is likely because the PA signals gradually change from cylindrical waves to spherical waves, and the spherical waves diverge much faster than the cylindrical waves. The top transducer does not show similar signal decrease, because the wave traveling upwards always follow the spherical shape. Nevertheless, it is clear that the side transducer is advantageous over the top transducer in detecting the PA signals from weakly-absorbing targets.

To further study the orientation dependence of the nonlinear effect on weak optical absorption, we simulated seven identical ultrasound transducers distributed in a half circle around the laser beam with a 30-degree interval, as shown in Fig. 4a. All transducers pointed to the optical focus and recorded the acoustic waves propagating in different directions. The optical absorption coefficient of the target was 0.1 cm$^{-1}$. Previously, we demonstrated that increasing the optical NA of OR-PAM could mitigate the limited view issue [15]. Here, to further investigate the impact of the optical beam shape on detecting weakly absorbing

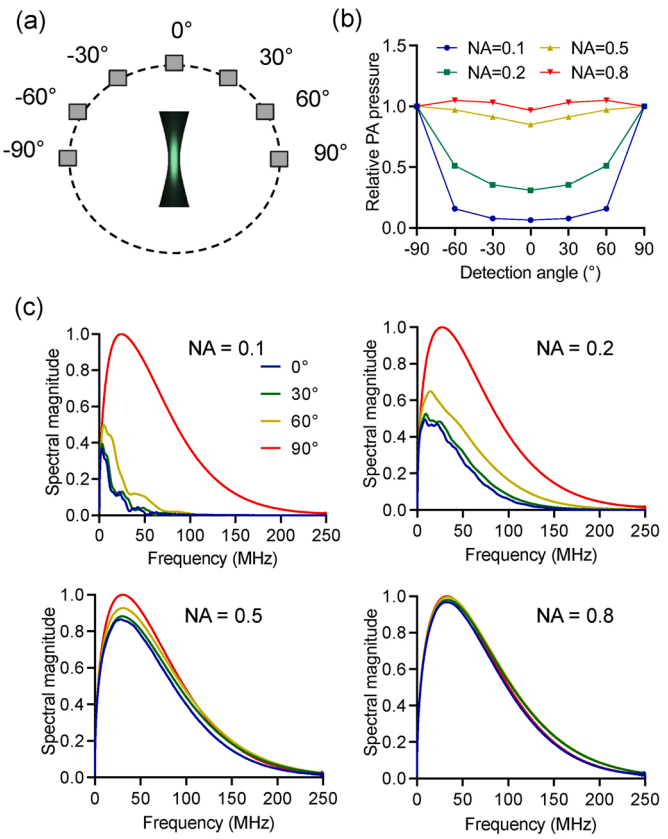


**Fig. 4.** Simulation of the orientation dependence of the PA signals with weak optical absorption. (a) Schematics of seven ultrasound transducers with unlimited bandwidth, distributed at different orientations pointing at the optical focus. The target has an optical absorption coefficient of 0.1 $cm^{-1}$. (b) The PA signal amplitudes recorded at different orientations, with the optical NA varying from 0.1 to 0.8. (c) Frequency spectra of the PA signals travelling at different orientations, with the optical NA varying from 0.1 to 0.8. All the spectra are normalized by the peak magnitude at 90°.

targets, we varied the optical NA of the laser beam from 0.1 to 0.8. As shown in Fig. 4b, for low optical NAs of 0.1 and 0.2, the top transducer at 0° received much weaker PA signals than the transducers on the sides (−90° and 90°), mainly because the low optical absorption and low optical NAs lead to cylindrical waves propagating sideways. Varying the detection orientations from 0° to 60° resulted in only slight improvement in signal amplitude, further confirming the side-propagating waves. However, with larger optical NAs of 0.5 and 0.8, the PA signal amplitudes detected at different orientations had significantly less difference, because these larger optical NAs lead to the generation of spherical waves propagating isotropically. Since most of the OR-PAM setups are implemented in the reflection mode, we have not simulated the 180-degree condition. In this case, the optical focal volume is asymmetric along the beam axis, and thus the transducer on top and at the bottom would detect opposite signal profiles along the time axis. Nevertheless, the signal non-linearity remains the same, since the side-travelling PA waves from weak absorbers are not well received in both 0-degree and 180-degree conditions.

In Fig. 4c, we also performed frequency analysis of the PA waves travelling at each orientation with different optical NAs. The results have collectively shown that when the optical NA is low (0.1 and 0.2), the signal frequencies have strong orientation dependence. The top transducer receives much lower frequencies than the side transducers, which could easily fall out of the detection bandwidth. However, such orientation dependence is much reduced as the optical NA increases, because the tightly focused light generates spherical-like waves, even with weak optical absorption. In summary, the results above show that the limited view is the dominating factor for the reduced detection sensitivity for the weak absorbers, while the limited detection bandwidth is the dominating factor for the saturation effect for the strong absorbers. Therefore, we propose that a side detection scheme or a high optical NA may provide a practical solution to mitigate the low detection sensitivity of OR-PAM on weakly absorbing targets.

## 3. Experimental validation

To validate the above nonlinear effect in OR-PAM, we performed phantom experiments using a reflection-mode OR-PAM system modified from our previous publication [33]. In the OR-PAM system (Fig. 5a), the

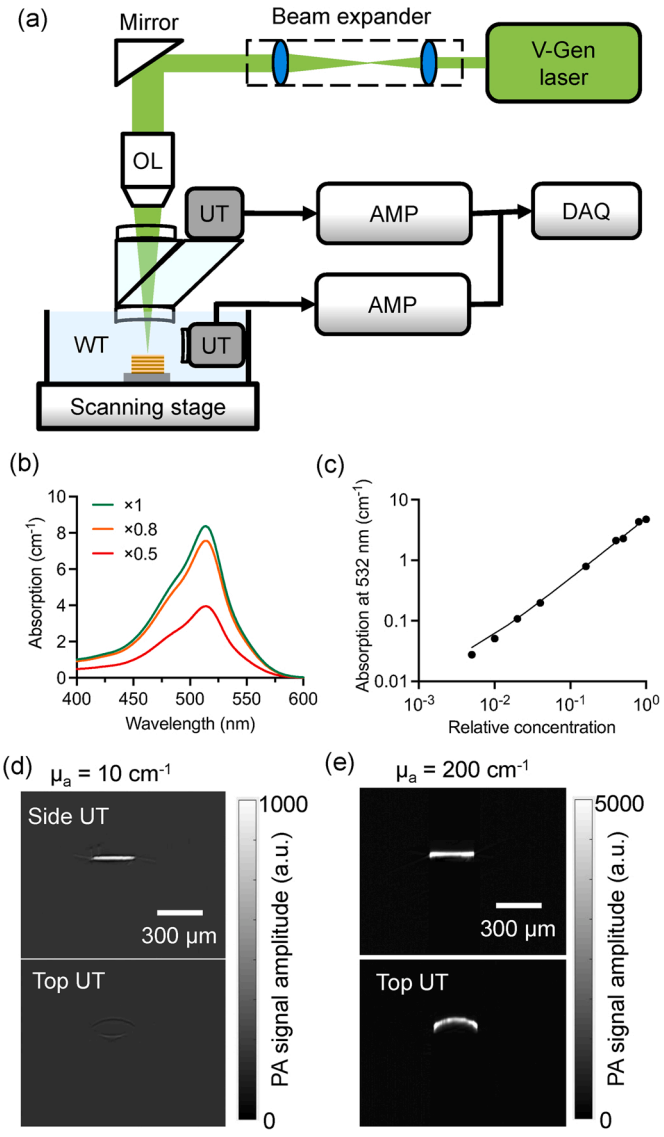


**Fig. 5.** Experimental validation of the OR-PAM's nonlinear dependence on optical absorption. (a) Schematic of the OR-PAM system with top and side ultrasound detection. AMP, amplifier; DAQ, data acquisition card; OL, objective lens; UT, ultrasound transducer; WT, water tank. (b) The absorption spectrum of the red ink solution with 400 ×, 500 ×, and 800 × dilutions. (c) The measured absorption coefficients at 532 nm of the red ink solutions with different dilutions. (d-e) Representative cross-sectional images (B-scan) of the tube acquired by the top and side transducers with weak (10 $cm^{-1}$) and high (200 $cm^{-1}$) optical absorption, respectively. (For interpretation of the references to colour in this figure legend, the reader is referred to the web version of this article.)

excitation light sources is an Nd: YAG laser (BX-60, Edgewave, Inc.). The laser light at 532 nm is focused by an objective lens (AC127–200-A, Thorlabs, Inc.) with an optical NA of 0.1. The top ultrasound transducer (V213, Olympus, Inc.) is confocally and coaxially aligned with the laser beam via an acoustic-optical combiner made of two prisms sandwiching a silicone oil layer. The side transducer (V213, Olympus, Inc.) is placed horizontally with the acoustic axis confocally aligned with the optical focus. Both transducers have a central frequency of 30 MHz, a detection bandwidth of 100%, and a focal length of 6 mm [14]. The detected PA signals by the top and side transducers are individually amplified and sampled. A two-dimensional motorized stage provides raster scanning of the sample. We used a 300-μm-diameter tube filled with red ink solutions (Dryden Designs) solutions as the absorbing sample, which had a peak absorption at 513 nm (Fig. 5b). The tube is made of PVC (polyvinyl chloride), with a wall thickness of 150 μm. The PVC is optically and acoustically transparent, and should not have significant impact on the PA signal generation and transmission. It is worth noting that in pactical in vivo applications, the blood vessel' wall thickness varies, or some chromophores are even without walls, which nevertheless doesn't influence the nonlinear dependence in this study. We prepared fifteen different ink solutions with the absorption coefficients varying from 0.2 $cm^{-1}$ to 190.5 $cm^{-1}$ (Fig. 5c). Different ink solutions were imaged in a random order.

The cross-sectional PA images (B-scans) of the ink-filled tube were averaged 500 times to improve the signal to noise ratio, particularly with weak optical absorption (Fig. 5d-e). The experimental results show that with weak optical absorption of 10 $cm^{-1}$ (Fig. 5d), the PA signals received by the top transducer was ~8 times weaker than that by the side transducer. Without signal averaging, it would be very challenging for the top transducer to detect such a weakly-absorbing target, but the side transducer was able to image the same target. By contrast, with strong optical absorption of 190 $cm^{-1}$ (Fig. 5e), the PA signals detected by the top transducer was only 25% weaker than that by the side transducer, which is approximately consistent with the simulation results.

We quantified the PA signal amplitudes at various optical absorption coefficients (Fig. 6a). The results by the side transducer showed a saturation effect with increasing absorption coefficients, mostly due to the limited detection bandwidth. A thresholding effect was observed for the top transducer detection when the optical absorption coefficient was lower than 20 $cm^{-1}$ (Fig. 6a). Such thresholding effect was not observed in the side transducer detection. Samples with low optical absorption generated side-propagating acoustic waves that were not efficiently detected by the top transducer, but well detected by the side transducer (Fig. 6b). Since the two detection paths (top and side) use the same model of ultrasound transducers and the acoustic focusing lens, the major difference is the beam-combiner with two prisms sandwiching a layer of silicone oil. The acoustic attenuation coefficient of the prism is approximately 3.6 nepers $m^{-1}$ at 30 MHz, indicating negligible attenuation in the prism over the detection path length. The prism-oil interface has a reflectivity of > 99%. The acoustic mode conversion at the prism-oil interface causes a signal loss of ~10%. Therefore, the ultrasound attenuation inside the beam combiner should be around 10%, which is close to what we observed in the result at $\mu_a = 200$ $cm^{-1}$ (Fig. 6a). The arrival time difference in Fig. 6b is because the beam combiner has a different speed of sound. Although arrival time difference exists, the raw PA signals detected from both top and side transducers show high similarity with large overlap in waveform shown in Fig. 6b (inset), where high absorption can be approximated as point source.

We further analyzed the acoustic frequencies of the detected PA signals for both transducers (Figs. 6c and 6d). The results demonstrated that the top transducer received more low-frequency waves when the optical absorption is low, which again, is consistent with the simulations results. More sensitive detection was achieved by the side transducer with weak optical absorption. Overall, the phantom experimental results have confirmed that there exists strong nonlinear dependence on the optical absorption in OR-PAM, majorly resultant from the limited view and detection bandwidth, which are both consistent with the simulation results.

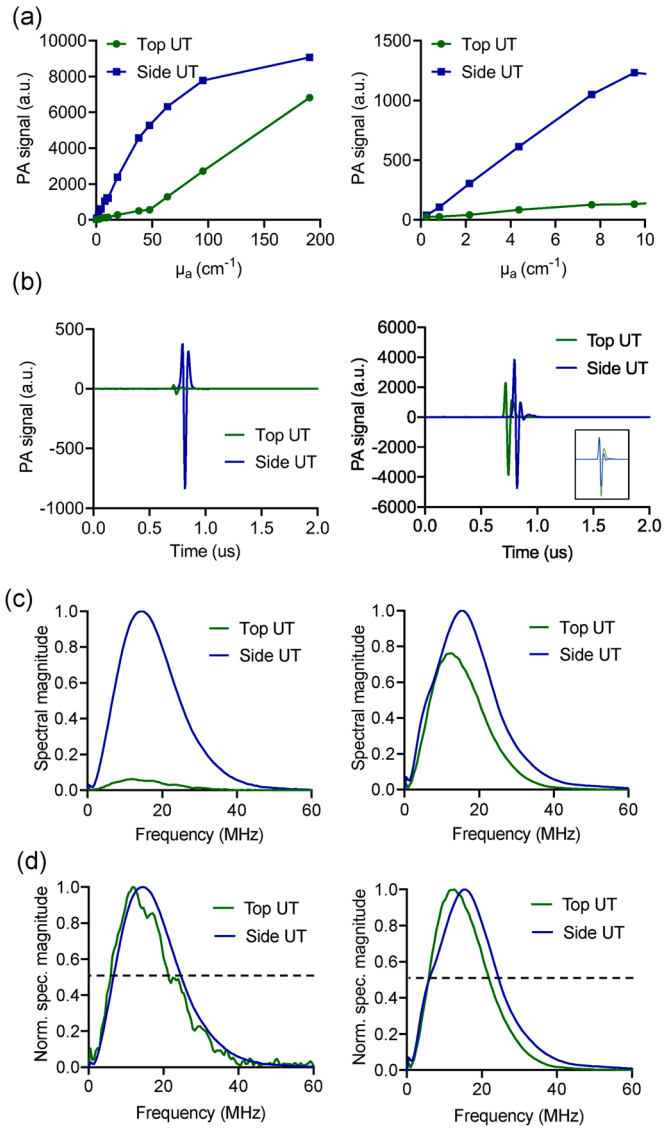


**Fig. 6.** Experimental validation results on the PA signal's nonlinear dependence on optical absorption. (a) PA signal amplitudes from red ink solutions with various optical absorption coefficients, detected by the top and side transducers. The plot on the right is a close-up plot with weak optical absorption of < 10 $cm^{-1}$. (b) Representative time-resolved RF signals detected by the top and side transducers, with an optical absorption of 10 $cm^{-1}$ (left) and 190 $cm^{-1}$ (right). The inset plot shows the signals after alignment. (c) The acoustic frequency spectra of the RF signals in (b), normalized by the side-transducer spectrum. (d) The acoustic frequency spectra of the RF signals in (b), normalized by the spectrum of each transducer itself, where the dotted lines indicating the − 6 dB bandwidth. (For interpretation of the references to colour in this figure legend, the reader is referred to the web version of this article.)

## 4. Conclusion and discussion

In this paper, we have investigated the PA signal generation and detection in a typical OR-PAM system with a low optical NA and weakly-absorbing target. Different from traditional understanding, our numerical simulation results have demonstrated a clear nonlinear signal dependence on optical absorption in OR-PAM, mainly due to the combined effect of limited detection view and detection bandwidth. The

ultrasound transducer placed coaxially with the laser beam has low efficiency in capturing the acoustic waves generated by low-NA optical beam and weakly-absorbing targets. Most of the acoustic waves travel sideways from the laser beam (i.e., limited view), and the much weaker acoustic waves traveling along the laser beam axis have low frequencies beyond the transducer's detection bandwidth (i.e., limited bandwidth).

We have also studied the impact of the optical NA on the detection of weak optical absorption. We have found that increasing the optical NA can help mitigate both the limited view and limited bandwidth issue, and thus improve the detection of weak absorption. Lastly, our experiments using dual-transducer OR-PAM have confirmed the simulation results. We conclude that the traditional OR-PAM system with a low optical NA does not have linear dependence on the optical absorption of weakly-absorbing targets.

As we have shown in the simulation results, the effective target shape is critical for the detection sensitivity of OR-PAM, which is mainly determined by the optical focal spot size and the optical absorption of the target. The total impulse response (TIR) of a transducer is also an important factor for PA signal detection sensitivity and spatial resolution of PAM [38–40], particularly when the signals are originating from out-of-focus region of the transducer. Correcting TIR may help improve the detection sensitivity if the effective target shape is known, which, however, is usually not available in practice. Although the signal nonlinearity in this work is only studied on a typical OR-PAM setup with a spherically focused transducer, the non-linear phenomenon should also exist for other transducer shapes such as flat, cylindrical, or Bessel-focused transducers.

Furthermore, the penetration depth of OR-PAM is usually limited to less than 1 mm, but other PAM implementations may reach to several millimeters. The non-linear effect studied in this work is unique to OR-PAM, because the effect target size is determined by the optical illumination pattern, instead of the true target geometry. The current work can be improved by translating the 2D k-wave simulation into 3D simulation. In the k-wave simulation of this work, we used a 2D detection geometry, in which the cylindrical wave was similar to a planar wave. The planar wave has slower divergence than the true cylindrical wave, which might explain the difference between the simulation and the experimental results. A 3D simulation can potentially address this issue.

For in vivo experiment, the detected PA signals are impacted by many factors such as the wavelength-dependent light attenuation and the frequency-dependent acoustic attenuation in the biological tissues. This work is mainly addressing one compounding factor that changes the PA signal's linear dependence on the optical absorption coefficient. Our results can provide better understanding on detecting weakly absorbing targets using OR-PAM, and is of great importance for functional and molecular imaging by OR-PAM, such as quantifying the blood oxygenation or the concentration of molecular probes. For example, oxyhemoglobin ($HbO_2$) and deoxy-hemoglobin (Hb) have significantly different absorption coefficients at NIR wavelength (e.g. at 680 nm, the difference is up to 10 times). In this case, the proposed nonlinear-dependence needs to be considered to improve the quantification accuracy of blood oxygenation.

OR-PAM defines the target shape by the effective optical beam pattern inside the target. In this case, simply increasing the excitation laser energy is not an effective way to improve the detection sensitivity. For the limited detection bandwidth in OR-PAM, one possible solution is to integrate multiple ultrasound transducers with complementary detection bandwidths. We have demonstrated a quad-mode PAM system, in which a dual-element transducer with complementary central frequencies was used to enhance the detection sensitivity [34]. For the limited detection view in OR-PAM, we have shown that increasing the optical NA can improve the visibility of vertical structures [15]. Moreover, novel image processing methods based on machine learning have gained momentum in PA imaging, which have shown promising performance in addressing the limited detection bandwidth and detection view in PACT [35–37]. We expect that these new approaches may also be applied to mitigate the nonlinear effect in OR-PAM.

## Funding information

This work was partially supported by American Heart Association Collaborative Sciences Award (18CSA34080277); Chan Zuckerberg Initiative Grant 2020–226178 by Silicon Valley Community Foundation, USA. We thank Dr. Caroline Connor for editing the manuscript.

## Declaration of Competing Interest

The authors declare that they have no known competing financial interests or personal relationships that could have appeared to influence the work reported in this paper.

## References

[1] Paul Beard, "Biomedical photoacoustic imaging.", Interface Focus 1 (4) (2011) 602–631.
[2] Fei Gao, Xiaohua Feng, Yuanjin Zheng, "Advanced photoacoustic and thermoacoustic sensing and imaging beyond pulsed absorption contrast.", J. Opt. 18 (7) (2016), 074006.
[3] V. Ntziachristos, J. Ripoll, L.V. Wang, R. Weissleder, "Looking and listening to light: the evolution of whole-body photonic imaging.", Nat. Biotechnol. 23 (3) (2005) 313–320.
[4] Lihong V. Wang, "Multiscale photoacoustic microscopy and computed tomography.", Nat. Photonics 3 (9) (2009) 503–509.
[5] Lihong V. Wang, Song Hu, "Photoacoustic tomography: in vivo imaging from organelles to organs.", Science 335 (6075) (2012) 1458–1462.
[6] Lihong V. Wang, Junjie Yao, "A practical guide to photoacoustic tomography in the life sciences.", Nat. Methods 13 (8) (2016) 627–638.
[7] Shin-Yuan Su, Pai-Chi Li, "Photoacoustic generation using coded excitation." Photons plus ultrasound: imaging and sensing, Int. Soc. Opt. Photon. 7899 (2011).
[8] Leihong Zhang, Liujie Sun, Xiuhua Ma, "Characteristics of the photoacoustic signal excited by an intensity-modulated continuous-wave laser.", Laser Phys. Lett. 10 (5) (2013), 055601.
[9] Jan Laufer, Dave Delpy, Clare Elwell, Paul Beard, "Quantitative spatially resolved measurement of tissue chromophore concentrations using photoacoustic spectroscopy: application to the measurement of blood oxygenation and haemoglobin concentration.", Phys. Med. Biol. 52 (1) (2006) 141.
[10] Hao F. Zhang, Konstantin Maslov, Mathangi Sivaramakrishnan, Gheorghe Stoica, Lihong V. Wang, "Imaging of hemoglobin oxygen saturation variations in single vessels in vivo using photoacoustic microscopy.", Appl. Phys. Lett. 90.5 (2007), 053901.
[11] H.F. Zhang, K. Maslov, G. Stoica, L.V. Wang, "Functional photoacoustic microscopy for high-resolution and noninvasive in vivo imaging.", Nat. Biotechnol. 24.7 (2006) 848–851.
[12] Junjie Yao, V.Wang Lihong, "Photoacoustic microscopy.", Laser Photonics Rev. 7.5 (2013) 758–778.
[13] Lihong V. Wang, "Tutorial on photoacoustic microscopy and computed tomography.", IEEE J. Sel. Top. Quantum Electron. 14 (1) (2008) 171–179.
[14] Junjie Yao, V.Wang Lihong, "Sensitivity of photoacoustic microscopy.", Photoacoustics 2 (2) (2014) 87–101.
[15] W. Liu, Y. Zhou, M. Wang, L. Li, E. Vienneau, R. Chen, J. Luo, C. Xu, Q. Zhou, L. V. Wang, J. Yao, "Correcting the limited view in optical-resolution photoacoustic microscopy.", J. biophotonics 11 (2) (2018), e201700196.
[16] Chi Zhang, Konstantin Maslov, Lihong V. Wang, "Subwavelength-resolution label-free photoacoustic microscopy of optical absorption in vivo.", Opt. Lett. 35 (19) (2010) 3195–3197.
[17] Chi Zhang, I.Maslov Konstantin, Song Hu, Lihong V. Wang, Ruimin Chen, Qifa Zhou, K. Kirk, Shung. "Reflection-mode submicron-resolution in vivo photoacoustic microscopy, J. Biomed. Opt. 17 (2) (2012), 020501.
[18] Eric M. Strohm, S.L.Berndl Elizabeth, C.Kolios Michael, "High frequency label-free photoacoustic microscopy of single cells.", Photoacoust. 1. 3-4 (2013) 49–53.
[19] Ryan L. Shelton, Brian E. Applegate, "Off-axis photoacoustic microscopy.", IEEE Trans. Biomed. Eng. 57 (8) (2010) 1835–1838.
[20] Amos Danielli, I. Konstantin, Alejandro Garcia-Uribe Maslov, M. Amy, Chiye Li Winkler, Wang Lidai, Chen Yun, W. Gerald, I.I. Dorn, V. Lihong, Wang, "Label-free photoacoustic nanoscopy.", J. Biomed. Opt. 19 (8) (2014), 086006.
[21] Amos Danielli, Konstantin Maslov, Christopher P. Favazza, Jun Xia, Lihong V. Wang, "Nonlinear photoacoustic spectroscopy of hemoglobin.", Appl. Phys. Lett. 106 (20) (2015), 203701.
[22] Amos Danielli, P.Favazza Christopher, Konstantin Maslov, Lihong V. Wang, "Single-wavelength functional photoacoustic microscopy in biological tissue.", Opt. Lett. 36 (5) (2011) 769–771.
[23] Jing Wang, Tan Liu, Shuliang Jiao, Ruimin Chen, Qifa Zhou, K. Kirk Shung, Lihong V. Wang, Hao F. Zhang, Saturation effect in functional photoacoustic imaging, J. Biomed. Opt. 15 (2) (2010), 021317.
[24] Hsun-Chia Hsu, Lei Li, Junjie Yao, Terence T.W. Wong, Junhui Shi, Ruimin Chen, Qifa Zhou, Lihong V. Wang, "Dual-axis illumination for virtually augmenting the

detection view of optical-resolution photoacoustic microscopy.", J. Biomed. Opt. 23 (7) (2018), 076001.
[25] Xosé Deán-Ben, Luís, Daniel Razansky, "On the link between the speckle free nature of optoacoustics and visibility of structures in limited-view tomography.", Photoacoustics 4 (4) (2016) 133–140.
[26] Zijian Guo, Li Li, Lihong V. Wang, "On the speckle-free nature of photoacoustic tomography.", 9Part1, Med. Phys. 36 (2009) 4084–4088.
[27] Lihong V. Wang, Wu Hsin-I, Biomedical optics: principles and imaging, John Wiley & Sons, 2012.
[28] C.G.A. Hoelen, F.F.M. De Mul, "A new theoretical approach to photoacoustic signal generation, J. Acoust. Soc. Am. 106 (2) (1999) 695–706.
[29] Toshitaka Agano, M. Kuniyil Ajith Singh, Ryo Nagaoka, Awazu Kunio, "Effect of light pulse width on frequency characteristics of photoacoustic signal–an experimental study using a pulse-width tunable LED-based photoacoustic imaging system.", Int. J. Eng. Technol. 7 (4) (2018) 4300–4303.
[30] R.Stephen Davidson, King Doreen, "Effect of particle size on photoacoustic signal amplitude, Anal. Chem. 56 (8) (1984) 1409–1411.
[31] Ben T. Cox, C.Beard Paul, "Fast calculation of pulsed photoacoustic fields in fluids using k-space methods.", J. Acoust. Soc. Am. 117 (6) (2005) 3616–3627.
[32] Bradley E. Treeby, T.Cox Benjamin, "k-Wave: MATLAB toolbox for the simulation and reconstruction of photoacoustic wave fields.", J. Biomed. Opt. 15 (2) (2010), 021314.
[33] Maomao Chen, J. Hailey, Yuqi Tang Knox, Liu Wei, Nie Liming, Chan Jefferson, Yao Junjie, "Simultaneous photoacoustic imaging of intravascular and tissue oxygenation.", Opt. Lett. 44 (15) (2019) 3773–3776.
[34] Wei Liu, M.Shcherbakova Daria, Neel Kurupassery, Yang Li, Qifa Zhou, Vladislav V. Verkhusha, Junjie Yao, "Quad-mode functional and molecular photoacoustic microscopy.", Sci. Rep. 8 (1) (2018) 1–10.
[35] Johannes Schwab, Stephan Antholzer, Robert Nuster, Markus Haltmeier, "Real-time photoacoustic projection imaging using deep learning.", arXiv Prepr. arXiv 1801 (2018) 06693.
[36] Dominik Waibel, Janek Gröhl, Fabian Isensee, Thomas Kirchner, Klaus Maier-Hein, Lena Maier-Hein, "Reconstruction of initial pressure from limited view photoacoustic images using deep learning." In photons plus ultrasound: imaging and sensing, Int. Soc. Opt. Photonics, 2018 10494 (2018) 104942S.
[37] Andreas Hauptmann, Felix Lucka, Marta Betcke, Nam Huynh, Jonas Adler, Ben Cox, Paul Beard, Sebastien Ourselin, Simon Arridge, "Model-based learning for accelerated, limited-view 3-d photoacoustic tomography.", IEEE Trans. Med. Imaging 37 (6) (2018) 1382–1393.
[38] M. Seeger, D. Soliman, J. Aguirre, et al., Pushing the boundaries of optoacoustic microscopy by total impulse response characterization, Nat. Commun. 11 (2020) 2910.
[39] A. Rosenthal, V. Ntziachristos, D. Razansky, "Optoacoustic methods for frequency calibration of ultrasonic sensors," in IEEE Transactions on Ultrasonics, Ferroelectr., Freq. Control 58 (2) (2011) 316–326, doi: 0.1109/TUFFC.2011.1809.
[40] S. Kellnberger, D. Soliman, G.J. Tserevelakis, et al., Optoacoustic microscopy at multiple discrete frequencies, Light Sci. Appl. 7 (2018) 109, https://doi.org/10.1038/s41377-018-0101-2.

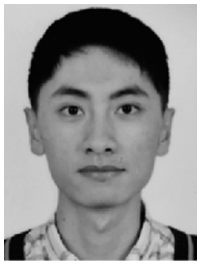

**Tingyang Duan** received the B.S. degree in microelectronics and solid state electronics from the University of Electronic Science and Technology of China, in 2016. He is currently a Ph. D. candidate at the School of Information Science and Technology, ShanghaiTech University. His current research interests focus on the development of PAM (photoacoustic microscope) imaging system and its biomedical applications.

**Xiaorui Peng** received her B.S. degree in Electrical Engineering from Beijing Institute of Technology in 2019 and her master's degree in Biomedical Engineering from Duke University in 2021. Now, Xiaorui joined the Optical Imaging Laboratory and is pursuing her Ph.D. degree in Biomedical Engineering at University of Michigan. Her current research interests focus on potential clinical applications of photoacoutics.

**Maomao Chen** is a postdoctoral research fellow in the BME department at Duke University. He received his Ph.D. degree from the Medical School of Tsinghua University, Beijing, China in 2017. His current research interest focuses on the system development and biological application of photoacoustic imaging.

**Dong Zhang** is currently a graduate student at Tsinghua University, China and a visiting scholar at Duke University, USA. His research interests are the development of novel biomedical imaging techniques including photoacoustic imaging and fluorescent molecular imaging.

**Fei Gao** received his bachelor degree in Microelectronics from Xi'an Jiaotong University in 2009, and PhD degree in Electrical and Electronic Engineering from Nanyang Technological University, Singapore in 2015. He worked as postdoctoral researcher in Nanyang Technological University and Stanford University in 2015–2016. He joined School of Information Science and Technology, ShanghaiTech University as an assistant professor in Jan. 2017, and established Hybrid Imaging System Laboratory (www.hislab.cn). During his PhD study, he has received Integrated circuits scholarship from Singapore government, and Chinese Government Award for Outstanding Self-financed Students Abroad (2014). His PhD thesis was selected as Springer Thesis Award 2016. He has published about 50 journal papers on top journals, such as Photoacoustics, IEEE TBME, IEEE TMI, IEEE JSTQE, IEEE TCASII, IEEE TBioCAS, IEEE Sens. J., IEEE Photon. J., IEEE Sens. Lett., ACS Sens., APL Photon., Sci. Rep., Adv. Func. Mat., Nano Energy, Small, Nanoscale, APL, JAP, OL, OE, JBiop, Med. Phys. He also has more than 60 top conference papers published in MICCAI, ISBI, ISCAS, BioCAS, EMBC, IUS etc. He has one paper selected as oral presentation in MICCAI2019 (53 out of 1700 submissions). In 2017, he was awarded the Shanghai Eastern Scholar Professorship. In 2018 and 2019, he received excellent research award from ShanghaiTech University. His interdisciplinary research topics include hybrid imaging physics, biomedical and clinical applications, as well as biomedical circuits, systems and algorithm design.

**Junjie Yao** is an assistant professor of Biomedical Engineering at Duke University, and a faculty member of Duke Center for In-Vivo Microscopy, Fitzpatrick Institute for Photonics, and Duke Cancer Institute. He received his B.E. and M.E. degrees at Tsinghua University, and his PhD in Biomedical Engineering at Washington University, St. Louis. His research interest is in photoacoustic tomography technologies in life sciences, especially in functional brain imaging and early cancer detection.